

# Author Manuscript

This is the author manuscript accepted for publication and has undergone full peer review but has not been through the copyediting, typesetting, pagination and proofreading process, which may lead to differences between this version and the [Version of Record](#). Please cite this article as [doi: 10.1002/fsb2.20953](https://doi.org/10.1002/fsb2.20953)

This article is protected by copyright. All rights reserved

Article type : Research Article

## **Toll-like receptor 2 (TLR2) engages endoplasmic reticulum stress sensor IRE1 $\alpha$ to regulate retinal innate responses in *S. aureus* endophthalmitis**

**Authors:** Ajay Kumar<sup>1</sup>, Pawan Kumar Singh<sup>1</sup>, Kezhong Zhang<sup>2, 3</sup>, and Ashok Kumar<sup>1, 3, #</sup>

### **Affiliations:**

<sup>1</sup>Department of Ophthalmology, Visual and Anatomical Sciences/ Kresge Eye Institute, Wayne State University School of Medicine, Detroit, MI, USA.

<sup>2</sup>Center for Molecular Medicine and Genetics, Wayne State University School of Medicine, Detroit, MI, USA.

<sup>3</sup>Department of Biochemistry, Microbiology, and Immunology, Wayne State University School of Medicine, Detroit, MI, USA.

<sup>4</sup>Department of Microbiology and Immunology, University of Michigan Medical School, Ann Arbor, MI, USA

**Running title:** IRE1 $\alpha$  regulates innate response in bacterial endophthalmitis

Corresponding Author: Ashok Kumar

Department of Ophthalmology, Visual and Anatomical Sciences

Wayne State University School of Medicine

4717 St. Antoine, Detroit, MI 48201

Tel: (313) 577-6213

E-mail: [akuma@med.wayne.edu](mailto:akuma@med.wayne.edu)

## ABSTRACT

Endoplasmic reticulum (ER) stress response has been implicated in a variety of pathophysiological conditions, including infectious and inflammatory diseases. However, its contribution in ocular bacterial infections, such as endophthalmitis, which often cause blindness is not known. Here, using a mouse model of *Staphylococcus (S.) aureus* endophthalmitis, our study demonstrates the induction of inositol-requiring enzyme 1 $\alpha$  (IRE1 $\alpha$ ) and splicing of X-box binding protein-1 (*Xbp1*) branch of the ER-stress pathway, but not the other classical ER stress sensors. Interestingly, *S. aureus* induced ER stress response was found to be dependent on Toll-like receptor 2 (TLR2), as evident by reduced expression of IRE1 $\alpha$  and *Xbp1* mRNA splicing in TLR2 knockout mouse retina. Pharmacological inhibition of IRE1 $\alpha$  using 4 $\mu$ 8C or experiments utilizing IRE1 $\alpha^{-/-}$  macrophages revealed that IRE1 $\alpha$  positively regulates *S. aureus* induced inflammatory responses. Moreover, IRE1 $\alpha$  inhibition attenuated *S. aureus*-triggered NF- $\kappa$ B, p38, and ERK pathways activation and cells treated with these pathway-specific inhibitors reduced *Xbp1* splicing, suggesting a positive feedback inhibition. *In vivo*, inhibition of IRE1 $\alpha$  diminished intraocular inflammation and reduced PMN infiltration in mouse eyes, but, increased bacterial burden and caused more retinal tissue damage. These results revealed a critical

role of the IRE1 $\alpha$ /XBP1 pathway as a regulator of TLR2 mediated protective innate immune responses in *S. aureus* induced endophthalmitis.

**KEY WORDS:** *S. aureus*, Endophthalmitis, Retina, Microglia, Reactive oxygen species (ROS), Inflammation, Endoplasmic reticulum (ER) stress, Toll-like receptor 2 (TLR2).

## ABBREVIATIONS

TLR2, Toll-like receptor 2; ER, Endoplasmic reticulum; IRE1 $\alpha$ , Inositol-requiring enzyme 1 $\alpha$ ; XBP1, X-box binding protein-1; NF- $\kappa$ B, Nuclear factor kappa-light-chain-enhancer of activated B cells; ROS, Reactive oxygen species; UPR, Unfolded protein response; PERK, protein kinase RNA-like ER kinase; ATF6, activating transcription factor 6; RNA, Ribonucleic acid; WT, Wild type; DLAR, Division of laboratory animal resources; ARVO, Association for Research in Vision and Ophthalmology; DMEM, Dulbecco's Modified Eagle Medium; FBS, fetal bovine serum; MOI, Multiplicity of infection; BMDM, Bone marrow derived macrophages; mM, millimolar; EDTA, Ethylenediaminetetraacetic acid; M-CSF, Macrophage colony-stimulating factor; PCR, Polymerase Chain reaction; ELISA, Enzymelinked immunosorbent assay; TNF $\alpha$ , tumor necrosis factor-alpha; IL-1 $\beta$ , Interleukin-1beta; IL6, Interleukin-6; MIP2, Macrophage Inflammatory Protein 2; CXCL2, Chemokine (C-X-C motif) ligand 2; KC, Keratinocyte chemoattractant; CXCL1, chemokine (C-X-C motif) ligand 1; TUNEL, Terminal deoxynucleotidyl transferase dUTP nick end labeling; H&E, hematoxylin and eosin; PMN, Polymorphonuclear cells; BSA, Bovine serum albumin; HRP, Horseradish peroxidase; LPS, Lipopolysaccharides; SA, *S. aureus*; LTA, Lipoteichoic acid; PGN, Peptidoglycan.

## 1 INTRODUCTION

2 *Staphylococcus (S) aureus* has long been recognized as an important bacterial pathogen  
3 causing various human diseases including infection of the bloodstream, skin, bone and  
4 joints as well as pneumonia (1-3). Aside from the aforementioned manifestations, *S. aureus*  
5 remains the leading cause of ocular diseases, such as bacterial endophthalmitis, which  
6 often results in poor prognosis even after treatment (4). Mostly, ocular trauma or surgical  
7 procedures predispose the eye to develop bacterial endophthalmitis (5, 6). Visual prognosis  
8 mainly depends on the virulence properties of the causative organism, visual ingenuity, and  
9 the efficacy of the antimicrobial treatment regime (7). Eye being an immunoprivileged  
10 organ, the retina is highly susceptible to host-induced inflammatory damage along with the  
11 injury caused by pathogens virulence factors. Previously, we have shown that retinal cells  
12 including Müller glia, microglia, and photoreceptors cells mount a massive innate immune  
13 response against *S. aureus* infection that could contribute to retinal damage in addition to  
14 providing protection against pathogen (8-10). Studies from both our laboratory and others  
15 have sought to elucidate the role of Toll-like receptors (TLRs) in the initiation of innate  
16 defense mechanisms in bacterial endophthalmitis (4, 8, 11-15). Of particular interest is  
17 TLR2, which has been found to orchestrate protective retinal innate immune responses in  
18 *Staphylococcal* endophthalmitis via modulating intraocular inflammation, and induction of  
19 antimicrobial peptides (4, 8-11, 15).

20 Endoplasmic reticulum (ER) is an intricate cellular organelle present in eukaryotic cells. The  
21 ER is a major site for protein synthesis and maturation and is involved in the processing of  
22 secretory and membrane proteins (16, 17). A wide variety of cellular conditions, including  
23 glucose deprivation, disruption of calcium homeostasis, and both viral and bacterial

24 infections, have been implicated as the causative agent behind the influx of unfolded or  
25 misfolded peptides which results in an ER stress response. To deal with this stress, the ER  
26 has evolved a set of signal transduction pathways that are collectively termed as unfolded  
27 protein response (UPR). For sensing ER stress, three major transmembrane transducers  
28 have been identified: Protein kinase RNA-like ER kinase (PERK), Inositol requiring enzyme  
29 (IRE1 $\alpha$ ), and activating transcription factor 6 (ATF6). Compared to other stress sensors,  
30 IRE1 $\alpha$  is the most conserved signaling branch. IRE1 $\alpha$  activation induces unconventional  
31 splicing of a 26-nucleotide intron from the RNA encoding X-box binding protein 1 (XBP1) to  
32 convert into mature XBP1s which then acts as a transcription factor (18). The IRE1 $\alpha$ -XBP1  
33 branch is evolutionary conserved from yeast to human and is essential for mammalian  
34 developmental processes (19). The cytoplasmic portion of IRE1 $\alpha$  has both kinase and  
35 endonuclease activities, whereas the luminal domain can detect unfolded proteins. The  
36 IRE1 $\alpha$  induced XBP1s then activates downstream genes, including the ER chaperones  
37 ERDj4, GRP78 (BiP), and PDI which are known to play a central role in restoring cellular  
38 ER homeostasis and promoting cell survival (20, 21). If ER stress is sustained for too long,  
39 it can result in persistent inflammation and eventual cell death (22).

40 Transcriptional induction of the *Xbp1* mRNA precursor after TLR stimulations in human  
41 macrophage, as well as mouse lung tissues during *Mycobacterium* and *Klebsiella* infection,  
42 have been reported (23, 24). ER stress response has been shown to either support or  
43 hamper disease progression by regulating inflammatory host defense pathways depending  
44 on the cell types, disease model, and the ER stressor (25). It has been shown that some  
45 intracellular pathogens utilize ER stress signaling as a protective mechanism for their  
46 intracellular growth and UPR induction is beneficial to the infection (26). Previously, TLR2

47 and TLR4 ligands mediated activation of ER stress response have been shown, which  
48 demonstrates a novel mechanism of IRE1 activation independent of protein misfolding in  
49 the ER lumen (27, 28). Nevertheless, the role of ER stress response in ocular infections,  
50 especially in bacterial endophthalmitis remains largely unexplored. Recently, we performed  
51 a transcriptomic analysis in *S. aureus* infected mouse retina (29) and discovered  
52 dysregulation of genes modulating ER stress response including *Xbp1* and *Bip*. Therefore,  
53 we initiated this study to investigate the role of ER stress in the bacterial ocular infection.

54 In the current study, we show that *S. aureus* infection in the eye specifically induces the  
55 IRE1 $\alpha$ /XBP1 axis of ER stress. Notably, we found that IRE1 $\alpha$  is essential for the induction  
56 of TLR2-mediated innate inflammatory responses and that the abrogation of this pathway is  
57 detrimental. In accordance, IRE1 $\alpha$  inhibition resulted in increased bacterial burden and  
58 retinal tissue damage in the eye. These results suggest that IRE1 $\alpha$ /XBP1 signaling is a  
59 protective host response in ocular infections.

## 60 **MATERIALS AND METHODS**

### 61 **Animals**

62 C57BL/6 [wild type (WT)] mice (both male and female, 6-8 weeks of age) were purchased  
63 from the Jackson Laboratory (Bar Harbor, ME). TLR2<sup>-/-</sup> breeders were purchased from  
64 Jackson Laboratory, bred in-house, and maintained in a pathogen-free, restricted-access  
65 Division of Laboratory Animal Resources (DLAR) facility at Kresge Eye Institute. *IRE1 $\alpha$ <sup>fllox/fllox</sup>*  
66 and myeloid cell-specific IRE1 $\alpha$ <sup>-/-</sup> mice (28) were provided by Dr. Kezhong Zhang (Center  
67 for Molecular Medicine and Genetics, Wayne State University). All animals were maintained

68 on a 12 h light 12 h dark cycle at 22°C temperature and provided free access to the tap  
69 water and LabDiet rodent chow (PicoLab; LabDiet, St. Louis, MO). All the procedures were  
70 conducted in compliance with the Association for Research in Vision and Ophthalmology  
71 (ARVO) statement for the Use of Animals in Ophthalmic and Vision Research and were  
72 approved by the Institutional Animal Care and Use Committee (IACUC) of Wayne State  
73 University.

#### 74 **Cell culture**

75 An immortalized mouse microglia (BV2) cell line was maintained in low-glucose Dulbecco's  
76 Modified Eagle Medium (DMEM) supplemented with 5% FBS and a penicillin-streptomycin  
77 cocktail (Invitrogen, Carlsbad, CA) in a humidified 5% CO<sub>2</sub> incubator at 37°C. Before  
78 treatment, cells were cultured in antibiotic-free and serum-free DMEM for 18 h (growth factor  
79 starvation). Cells were either stimulated with TLR agonist Pam3CysSK4 (10 µg/ml) or  
80 infected with *S. aureus* RN6390 multiplicity of infection (MOI) 10:1 for 8h.

#### 81 **Induction of *S. aureus* endophthalmitis**

82 Endophthalmitis was induced in mice as described previously (4, 10). Briefly, mice were  
83 anesthetized by intraperitoneal injection of ketamine/xylazine (ketamine, 100-125 mg/kg;  
84 xylazine, 10-12.5 mg/kg). Under an ophthalmoscope, mice left eyes were injected  
85 intravitreally with *S. aureus* strain RN6390 (5000CFU/eye) using a 34G needle attached to  
86 a 10µl syringe (WPI). Contralateral eyes injected with sterile PBS served as control. At the  
87 desired time points post-infection; enucleated eyes or neural retina were subjected to  
88 bacterial growth determination, inflammatory cytokines/ chemokines assays, Western  
89 blotting, and histology as described in the following sections.



## 90 **Isolation of bone marrow-derived macrophage (BMDM)**

91 Bone marrow-derived macrophages (BMDM) were isolated as described previously (30,  
92 31). Briefly, bone marrow cells from *IRE1α<sup>flox/flox</sup>* and myeloid cell-specific *IRE1α* KO mice  
93 were flushed from femurs and tibiae using RPMI media containing 10% FBS and 0.2 mM  
94 EDTA. RBCs were lysed by adding a hypotonic solution of 0.2% NaCl for 20 s, followed by  
95 the addition of 1.6% NaCl. Bone marrow cells were pelleted by centrifugation at 400 x g for  
96 5 min followed by a wash with RPMI media. Cells were resuspended, counted, and cultured  
97 in RPMI media supplemented with 10% FBS, 100 U/ml penicillin, 100 mg/ml streptomycin,  
98 and 10 ng/ml M-CSF at 37°C in 5% CO<sub>2</sub> for macrophage differentiation. Six days post-  
99 differentiation  $\sim 1 \times 10^6$  BMDM/ml were seeded in 6 well tissue-culture plates for *in-vitro*  
100 experiments.

## 101 **RNA extraction and Polymerase chain reaction (PCR)**

102 Total RNA was extracted from both mouse neural retina and BV2 cells using TRIzol per  
103 manufacturer's instructions (Invitrogen, Carlsbad, CA, USA). One microgram of total RNA  
104 was reversed transcribed using Maxima first-strand cDNA synthesis kit per manufacturer's  
105 instructions (Thermo Scientific, Rockford, IL, USA). cDNA was amplified for a gene of  
106 interest by PCR using mouse-specific primers. PCR products along with housekeeping  
107 internal control GAPDH, were subjected to electrophoresis on 2.5% or 1.2% agarose gel  
108 according to the size of the PCR amplicons. For XBP1 splicing detection, both, unspliced  
109 and spliced forms of XBP1 mRNA species were resolved using high-percentage (2.5%)  
110 agarose gel electrophoresis which is often used to detect *IRE1α* endonuclease activity.

111 Images of ethidium bromide-stained gels were captured using a digital camera (EDAS 290  
112 system, Eastman Kodak, Rochester, NY).

113  
114 **Enzyme-linked immunosorbent assay (ELISA)**

115 ELISA was performed to quantify the levels of cytokines/chemokines in mice ocular tissue  
116 as well as the cells conditioned media. Briefly, mouse eyes were enucleated and  
117 homogenized in sterile PBS by stainless steel beads using Tissue lyser (Qiagen, Valencia,  
118 CA) followed by centrifugation at 15,000 x g for 15 min. Total protein was estimated using  
119 the Micro BCA™ protein estimation kit (Thermo Scientific, Rockford, IL, USA) per  
120 manufacturer's instructions. ELISA was performed for tumor necrosis factor-alpha (TNF- $\alpha$ ),  
121 interleukin-1beta (IL-1 $\beta$ ), interleukin-6 (IL-6) (BD biosciences, San Diego, CA, USA) and  
122 macrophage inflammatory protein 2 (MIP2/CXCL2) and CXCL1/KC (R&D systems,  
123 Minneapolis, MN, USA) per manufacturer's instructions.

124 **Histology and Terminal deoxynucleotidyl transferase dUTP nick end labeling**  
125 **(TUNEL) assay**

126 Mice eyes were enucleated at desired time points for histopathological examination and  
127 fixed in 10% formalin. Embedding, sectioning and hematoxylin and eosin (H&E) staining  
128 were performed by Excalibur Pathology Inc. (Oklahoma City, OK, USA). All retinal H&E  
129 sections were observed with a light microscope (400 X magnification). For TUNEL staining,  
130 the eyes were fixed in Tissue-Tek OCT (Sakura, Torrance, CA, USA) and 6-8  $\mu$ m thick  
131 sagittal sections were collected from each eye and mounted onto microscope slides. Retinal

132 sections were used for the TUNEL staining using ApopTag® Fluorescein In situ Apoptosis  
133 Detection Kit according to the manufacturer's instruction (Millipore, Billerica, MA, USA).

#### 134 **Polymorphonuclear cells (PMNs) infiltration**

135 To determine the PMNs infiltration in mice retina, flow cytometry was used as described  
136 previously (32). Briefly, following euthanasia, retinas were isolated and digested with  
137 Accumax (Millipore, MA, USA) for 10 minutes at 37°C. A single-cell suspension was  
138 prepared by triturating the retina using a 23-G needle/syringe and filtered through a 40µm  
139 cell strainer (BD Falcon, San Jose, CA, USA). To reduce the non-specific binding of  
140 antibodies, cells were incubated with Fc Block (BD Biosciences) for 30 minutes. After  
141 washing with 0.5% BSA, cell suspensions were incubated with conjugated monoclonal  
142 antibodies CD45-PECy5, Ly6G-FITC, and respective isotype controls (BD Biosciences) in  
143 dark for 30 minutes. After washing, cells were acquired and analyzed using the Accuri C6  
144 flow cytometer and software (BD Biosciences, San Jose, CA, USA) respectively.

#### 145 **Immunoblotting**

146 For immunoblotting, cells were lysed using radioimmunoprecipitation (RIPA) lysis buffer  
147 containing a protease and phosphatase inhibitor cocktail (Thermo Scientific, Rockford, IL,  
148 USA). Mice neural retinas were lysed by sonication in PBS containing a protease and  
149 phosphatase inhibitor cocktail. Total protein concentration was determined, and 30-40 µg  
150 protein was used for blotting. Denatured proteins were resolved in a 12% SDS-  
151 polyacrylamide gel and transferred onto a nitrocellulose membrane (0.44µm) (Bio-Rad  
152 Laboratories). Following blocking, the blots were incubated with anti-phospho (Ser-51)-

153 IRE1 $\alpha$ , anti-total IRE1 $\alpha$  (1:1000) (Cell signaling Technology, Boston, MA) and anti- $\beta$ -actin  
154 (1:5000) (Sigma-Aldrich, St. Louis, MO) antibodies overnight at 4°C. Following washing,  
155 blots were incubated with goat anti-rabbit/ mice-IgG-HRP conjugate (BioRad, Hercules, CA).  
156 Protein bands were developed using SuperSignal West Femto Chemiluminescent Substrate  
157 and visualized using iBright FL1500 Imaging Systems (ThermoFisher Scientific, Rockford,  
158 IL).  $\beta$ -actin was used as a control for protein loading. Quantification of the intensity of bands  
159 was performed using ImageJ software (Rasband, W.S., ImageJ, U. S. National Institutes of  
160 Health, Bethesda, Maryland, <http://rsb.info.nih.gov/ij/>, 1997-2009).

## 161 **Immunostaining**

162 Immunostaining was performed as described earlier (33, 34). Briefly, cells were cultured on  
163 four well glass chamber slides (Fisher Scientific, Rochester, NY) and pre-treated with 4 $\mu$ 8C  
164 (IRE1 $\alpha$  inhibitor) 1h before *S. aureus* challenge. Following stimulation, cells were washed  
165 three time with PBS and fixed in 4% paraformaldehyde for 15 min. Cells were permeabilized  
166 with an ethanol: acetic acid mixture (2:1) at -20°C for 10 min. and washed. The fixed cells  
167 were blocked in 1% (w/v) BSA for 1h at room temperature followed by incubation with  
168 primary antibodies (1:100 dilution) overnight at 4°C. Cells were washed with PBS and  
169 incubated with specific fluorescein isothiocyanate (FITC)-conjugated secondary antibodies  
170 (1:200 dilutions) for 1h at room temperature. Following incubation cells were washed with  
171 PBS and mounted in Vectashield anti-fade mounting medium with DAPI (Vector  
172 Laboratories). Slides were visualized using an Eclipse 90i fluorescence microscope (Nikon,  
173 Melville, NY)

## 174 **Statistical analysis**

175 Statistical analysis was performed using GraphPad Prism V8 (GraphPad Software, La Jolla,  
176 CA). All data has been expressed as means  $\pm$  SD unless indicated otherwise. Unpaired  
177 student t-test or One-way ANOVA was used for comparisons followed by Dunnett's' posthoc  
178 test wherever applicable. A *P*-value of  $<0.05$  was considered statistically significant. All  
179 experiments were performed at least three time unless indicated otherwise.

180

## 181 RESULTS

### 182 ER stress is induced during *S. aureus* endophthalmitis

183 Bacterial infections have been shown to trigger an unfolded protein response (UPR) (35,  
184 36) resulting in the activation of the ER-transmembrane protein IRE1 $\alpha$ . Although multiple  
185 targets for the IRE1 $\alpha$  endonuclease have been identified, the splicing of *Xbp1* mRNA is  
186 the main under infectious and inflammatory conditions (37). To assess whether IRE1 $\alpha$ -  
187 XBP1 or other ER stress sensors are induced in bacterial endophthalmitis, we analyzed  
188 transcriptomic data that had been previously published (29). Indeed, our data showed a  
189 time-dependent induction of *XBP1* (**Fig 1A**, upper panel) and *BiP* (**Fig 1A**, lower panel)  
190 mRNA transcripts upon *S. aureus* infection by qRT-PCR. To further confirm our microarray  
191 data, we performed independent experiments and found *S. aureus* infection induced the  
192 expression of IRE1 $\alpha$  and the splicing of *XBP1* mRNA in mice retina, indicating the onset of  
193 ER stress response (**Fig 1B**). However, the expression of CHOP, WSF, ER-localized DnaJ  
194 homologue 4 (ERDj4), and the disulfide isomerase PDI did not change noticeably in infected  
195 retinal tissue as compared to control (**Fig 1B**), indicating that ATF6 and PERK pathways are

196 unlikely involved in *S. aureus* induced ER stress response in the retina (38, 39). These  
197 observations led us to focus on the IRE1 $\alpha$  mediated ER stress pathway in *S. aureus*  
198 endophthalmitis.

199 To evaluate the specificity of the bacterial-induced IRE1 $\alpha$ -XBP1 axis of ER stress we used  
200 a potent pharmacological inhibitor of IRE1 $\alpha$ , 4 $\mu$ 8C, which inhibits substrate access to the  
201 active site of IRE1 leading to the inactivation of *Xbp1* splicing and IRE1-mediated mRNA  
202 degradation (40). To investigate this, first, we performed a dose-response study using 4 $\mu$ 8C  
203 on mouse BV2 microglia cells (10) challenged with *S. aureus* (**Fig S1A**). Because all the  
204 dosages of 4 $\mu$ 8C tested showed a reduction of *XBP1* mRNA splicing (XBP1s), we decided  
205 to use 100 nM of this inhibitor for the remainder of the study.

## 206 ***S. aureus* induces IRE1 $\alpha$ mediated ER stress response via TLR2**

207 In the eye, *S. aureus* has been shown to invoke retinal innate responses through TLR2  
208 signaling (4, 10, 11) and TLRs have been implicated in triggering ER stress (26, 27), we  
209 sought to decipher the link between TLR2 and IRE1 $\alpha$  activation in our disease model, which  
210 is currently unknown. To establish the role of TLR2 signaling in regulating IRE1 $\alpha$  mediated  
211 ER stress response, *S. aureus* endophthalmitis was induced in wild type (WT) C57BL/6,  
212 TLR2<sup>-/-</sup>, and MyD88<sup>-/-</sup> mice with or without 4 $\mu$ 8C pretreatment. Our data shows *S. aureus*  
213 infection-induced activation of IRE1 $\alpha$  and prominent splicing of *Xbp1* transcripts in WT and  
214 MyD88<sup>-/-</sup> mice and the response was attenuated by 4 $\mu$ 8C treatment. In contrast, infected  
215 TLR2<sup>-/-</sup> mouse retina did not show the splicing of XBP1 (**Fig 2A**). We further confirmed the  
216 IRE1 $\alpha$  activation at protein levels in retinal tissue of *S. aureus* infected WT, TLR2<sup>-/-</sup> and  
217 MyD88<sup>-/-</sup> mice by western blotting. Our results show that *S. aureus* significantly induced the

218 phosphorylation of IRE1 $\alpha$  in WT and MyD88<sup>-/-</sup> mice whereas, its levels were significantly  
219 lower in TLR2<sup>-/-</sup> mice (**Fig 2B**). These results indicate that TLR2 mediates IRE1 $\alpha$ -mediated-  
220 ER stress response in *S. aureus* endophthalmitis.

221 For *in vitro* studies, we used mouse BV2 microglia which have been shown to respond to *S.*  
222 *aureus* challenge analogous to that of primary retinal microglia (10). To examine the role of  
223 TLRs in IRE1 $\alpha$  activation in our model, BV2 microglia were challenged with the TLR2  
224 agonist, Pam3CSK4, and the TLR4 agonist, LPS, in the presence and absence of IRE1 $\alpha$   
225 inhibitor 4 $\mu$ 8C; live *S. aureus* (SA) was used as a positive control. Our results show all  
226 agents (Pam3CSK4, LPS, and SA) induced the expression of IRE1 $\alpha$  as well as the splicing  
227 of *XBP1* and that this response was reduced by 4 $\mu$ 8C treatment (**Fig 2C**). We also examined  
228 the activation of classical ER-stress response and found no marked induction of CHOP,  
229 ERDj4, and PDI expression in response to the Pam3CSK or *S. aureus* challenge (**Fig 2C**).  
230 Induction of IRE1 $\alpha$  and its inhibition by 4 $\mu$ 8C was confirmed at the protein level by western  
231 blotting (**Fig 2D**) and immunostaining (**Fig S1B**), which displayed reduced phosphorylation  
232 of IRE1 $\alpha$  upon 4 $\mu$ 8C treatment in BV2 microglial cells.

233 In addition to specific TLR ligands, we assessed the effect of *S. aureus* virulence factors ( $\alpha$ -  
234 toxin, LTA, PGN) on ER stress response and observed that they also modestly induced the  
235 expression of IRE1 $\alpha$  and XBP1 splicing (**Fig S2A**).

### 236 **IRE1 $\alpha$ regulates *S. aureus* and TLR2 ligand-induced inflammatory response**

237 TLR mediated ER stress response has been linked to the elicitation of innate responses in  
238 various pathological conditions (27, 41, 42). Hyperglycemia-induced ER stress has also

239 been implicated in retinal Müller glia-derived inflammatory response in diabetic retinopathy  
240 (43). To assess the functional role of IRE1 $\alpha$  activation in *Staphylococcal* endophthalmitis,  
241 we evaluated inflammatory mediators in mice eyes and cultured BV2 microglial cells. As  
242 expected, *S. aureus* induced the production of key inflammatory cytokines, IL-1 $\beta$ , TNF- $\alpha$ ,  
243 and the chemokine MIP2 in retinal tissue, whereas their levels were significantly reduced in  
244 mouse eyes pre-treated with the IRE1 $\alpha$  inhibitor 4 $\mu$ 8C (**Fig 3A**). Similarly, pretreatment of  
245 BV2 microglia with 4 $\mu$ 8C significantly attenuated inflammatory mediators induced by *S.*  
246 *aureus* and Pam3CSK4 (**Fig 3B**).

247 Next, to further solidify the role of IRE1 $\alpha$  in an *S. aureus* induced inflammatory response,  
248 we used bone marrow-derived macrophages (BMDM) from IRE1 $\alpha^{\text{flox/flox}}$  and myeloid cell-  
249 specific IRE1 $\alpha^{-/-}$  mice. *S. aureus* challenge of IRE1 $\alpha^{\text{flox/flox}}$  BMDM resulted in robust  
250 production of pro-inflammatory cytokines (IL-1 $\beta$ , TNF- $\alpha$ , and IL-6) but this was not the case  
251 in IRE1 $\alpha^{-/-}$  BMDM (**Fig 3C**). Collectively, these results support the hypothesis that IRE1 $\alpha$   
252 mediates an innate inflammatory response in both *Staphylococcal* endophthalmitis and  
253 cultured immune cells (microglia and macrophages).

#### 254 **Inhibition of IRE1 $\alpha$ attenuates *S. aureus* induced NF- $\kappa$ B and MAPK signaling**

255 Because NF- $\kappa$ B and other MAP kinases, such as ERK and p38 are known to regulate the  
256 inflammatory response in *S. aureus* endophthalmitis (10, 30, 44), we decided to assess their  
257 link with IRE1 $\alpha$  activation (45). *Staphylococcal* endophthalmitis was induced in WT mouse  
258 eyes pretreated with 4 $\mu$ 8C, and western blot was performed to detect I $\kappa$ B and MAPKs in  
259 retinal tissue lysates. Our results show that *S. aureus* induced phosphorylation of I $\kappa$ B,  
260 ERK1/2, and p38 proteins, whereas, IRE1 $\alpha$  inhibition reduced the activation of these



261 signaling molecules (**Fig 4A**). Similarly, the pathway-specific inhibitors for I $\kappa$ B, ERK1/2, and  
262 p38 reduced *S. aureus*-induced *Xbp1* splicing (**Fig 4B**), indicating the existence of a  
263 feedback inhibition system among these pathways. The activity of these pathway inhibitors  
264 was validated by assessing *S. aureus* induced mRNA expression of the inflammatory  
265 cytokine *Il-1 $\beta$*  (**Fig S2B**). Together, these results suggest that IRE1 $\alpha$  is an upstream  
266 regulator of *S. aureus*-induced NF- $\kappa$ B and MAPKs signaling.

### 267 ***S. aureus* induced ROS activates IRE1 $\alpha$ -XBP-mediated ER stress response**

268 A correlation between ROS generation and the induction of ER stress has been shown in  
269 several pathological conditions (46-48). Previously, we have shown that *S. aureus* induces  
270 ROS generation in retinal cells (9). Therefore, we sought to investigate whether *S. aureus*  
271 induced ROS production plays any role in the IRE1 $\alpha$  mediated ER stress response. To  
272 investigate this, we used Diphenyleneiodonium (DPI), an NAD(P)H oxidase inhibitor, and a  
273 potent ROS blocker. Our data showed DPI pretreatment in BV2 microglia, reduced *S.*  
274 *aureus*-triggered IRE1 $\alpha$  expression as well as *Xbp1* splicing (**Fig 5A**). Moreover, the  
275 conditioned media from DPI treated cells showed reduced accumulation of inflammatory  
276 mediators (**Fig 5B**). This observation indicates that *S. aureus*-induced ROS generation  
277 contributes to the induction of ER stress, and blocking ROS production could prevent *S.*  
278 *aureus*-induced ER stress.

### 279 **IRE1 $\alpha$ inhibition results in increased bacterial burden and tissue damage in the eye**

280 ER stress can either promote or impede disease progression depending on the disease  
281 model, cell types, and the ER stress sensors involved (49-51). Studies have shown that

282 some intracellular pathogens use ER stress signaling as a protective mechanism for their  
283 intracellular growth, making IRE1 $\alpha$  induced UPR beneficial for the spread of infection (25,  
284 52, 53). Since found that *S. aureus* induced IRE1 $\alpha$  activation and *Xbp1* splicing both *in vivo*  
285 and *in vitro*, and IRE1 $\alpha$  inhibition diminished pro-inflammatory cytokine production, we  
286 sought to determine the effect of IRE1 $\alpha$  inhibition (4 $\mu$ 8C treatment) on disease progression.  
287 First, we assessed the intraocular bacterial burden, and unexpectedly, we found that IRE1 $\alpha$   
288 inhibition resulted in higher bacterial load in the eyes as compared to *S. aureus* alone  
289 injected eyes. (**Fig 6A**). To assess *S. aureus*-induced disease pathology, we performed  
290 histological analysis and our data showed increased retinal damage (retinal folding and  
291 disintegration of retinal layers), and fibrin formation in 4 $\mu$ 8C-treated eyes compared to eyes  
292 only infected with *S. aureus* (**Fig 6B**). This observation was confirmed by TUNEL staining  
293 of retinal sections which showed more TUNEL positive cells in eyes treated with the IRE1 $\alpha$   
294 inhibitor, 4 $\mu$ 8C (**Fig 5C**), indicating increased retinal cell death. We also performed flow  
295 cytometry to assess PMN infiltration and found significantly reduced PMN infiltration in the  
296 retina upon IRE1 $\alpha$  inhibition (**Fig 6D**). Altogether, these results indicate that IRE1 $\alpha$ -mediated  
297 ER stress is essential in controlling disease pathology in bacterial endophthalmitis.

298

## 299 **DISCUSSION**

300 This study demonstrates that IRE1 $\alpha$ /XBP1 axis of ER stress pathways plays a pivotal role  
301 in the eye during bacterial (*S. aureus*) endophthalmitis through regulation of innate  
302 inflammatory responses. The pharmacological inhibition of this pathway markedly increased  
303 disease severity by increasing bacterial proliferation and more retinal tissue damage in the

304 eye. Most importantly, we found that bacterial-induced IRE1 $\alpha$ /XBP1 signaling was TLR2  
305 dependent. Since the attenuation of ER stress has been mostly shown beneficial in eye  
306 diseases (54-56), our study reveals what we believe an unconventional role for the  
307 IRE1 $\alpha$ /XBP1 pathway as a crucial regulator of ocular innate immunity (**Fig 7**).

308 Our rationale of the current study emerged from an earlier transcriptomics analysis (29),  
309 showing induced expression of *Xbp1* and *Bip* transcripts in *S. aureus* infected mouse retina,  
310 indicating their role in the pathobiology of bacterial endophthalmitis. Although several ER  
311 stress pathways can be triggered in mammalian cells under infectious and inflammatory  
312 conditions, we did not observe the activation of ATF6 or the PERK pathway. We therefore,  
313 hypothesized that the primary pathway involved in our disease model is the IRE1 $\alpha$ -XBP1  
314 pathway. This is supported by multiple pieces of evidence, including, splicing of IRE1 $\alpha$   
315 downstream target XBP1 and the attenuation of an inflammatory response and severe  
316 disease pathology by pharmacological inhibition of IRE1 $\alpha$ . These observations corroborate  
317 with studies where activation of IRE1-XBP1 mediated ER stress has also been reported via  
318 various intracellular pathogens such as *Chlamydia trachomatis* (57), *Brucella abortus* (58)  
319 and *Francisella tularensis* (27). However, some other bacterial species and their toxins such  
320 as subtilase toxin produced by *Escherichia coli* (59), and listeriolysin O, produced by *Listeria*  
321 *monocytogenes* (60) have been shown to activate other arms of the UPR as well. In addition  
322 to live *S. aureus* infection, we found that TLR2 ligand, Pam3CSK4, and other *S. aureus*  
323 virulence factors (PGN, LTA,  $\alpha$ -toxin) also activate the IRE1-XBP1 pathway, indicating the  
324 potential involvement of TLR2 signaling in regulating an IRE1 mediated ER stress response.  
325 Moreover, LPS induced IRE1 $\alpha$  activation through TRAF6 has also been reported by Zhang  
326 and co-workers in collaboration with our laboratory (61). Consistent with our data, other

327 studies have suggested that TLR2 can activate the IRE1 $\alpha$  pathway, but not the ATF6 or  
328 PERK pathways (27).

329 Furthermore, we established the role of TLR2 signaling in *S. aureus* induced ER stress using  
330 TLR2 and its downstream adaptor, MyD88 deficient mice. We found that *S. aureus* induced  
331 IRE1 $\alpha$ -mediated ER stress is TLR2 dependent but only partially dependent on MyD88  
332 pathways. Prior reports have shown impaired XBP1 splicing in TLR2-deficient macrophages  
333 following TLR2 agonists Pam3CSK4, FSL1, *F. tularensis* challenge and MRSA infection (27,  
334 47). Similarly, *Xbp1* splicing has been reported in macrophages by both MyD88 dependent  
335 and independent mechanisms(27). Both TLR-signaling and IRE1-mediated splicing of *Xbp1*  
336 have been shown to invoke innate immune responses and the production of inflammatory  
337 cytokines (27, 36, 47, 62). Our data demonstrated that inhibiting IRE1 $\alpha$  attenuates *S. aureus*  
338 induced cytokine production *in vivo* (mouse model of endophthalmitis) as well as in cultured  
339 microglia, implicating its role in regulating the inflammatory innate immune response. The  
340 experiments using BMDM from myeloid cell-specific IRE1<sup>-/-</sup> mice further validates these  
341 findings by showing inhibition of *S. aureus* induced inflammatory mediators. Thus, we  
342 conclude that TLR2 triggers IRE1 $\alpha$  activation to initiate an innate immune response in *S.*  
343 *aureus* endophthalmitis.

344 Previous studies from our laboratory and other investigators have shown that in ocular  
345 infections, NF- $\kappa$ B and MAPK activation are key players in orchestrating inflammatory  
346 responses by various retinal cell types (10, 30, 44). In this study, we demonstrated that in  
347 response to *S. aureus* infection, IRE1 $\alpha$  mediated ER stress controls the activation of NF-  
348  $\kappa$ B, and MAPK such ERK, and p38 signaling pathways. Similarly, the inhibition of these pro-

349 inflammatory signaling pathways by using their pharmacological inhibitors, resulted in  
350 impaired splicing of *Xbp1*, suggesting positive feedback inhibition of ER stress. These  
351 results indicate that diminished pro-inflammatory cytokines production upon IRE1 inhibition  
352 could be due to the downregulation of *S. aureus* induced NF- $\kappa$ B and MAPK activation.

353 Reactive oxygen species (ROS) production and ER stress induction are a part of a positive  
354 feedback loop(47, 63). Innate immune cells also utilize ROS to kill pathogens, including *S.*  
355 *aureus* (9, 47). We previously showed *S. aureus* infection lead to ROS production in retinal  
356 cells (9). Our experiment utilizing NADPH oxidase inhibitor, DPI, resulted in reduced *Xbp1*  
357 splicing and diminished production of inflammatory cytokine, establishes a link between  
358 ROS generation and IRE1 $\alpha$  activation (47). Our data showed an increased bacterial burden  
359 in the eyes upon IRE1 $\alpha$  inhibition, indicating that IRE1 $\alpha$ -mediated ER stress contributes  
360 towards antibacterial activity. Since we observed reduced PMN infiltration in eyes treated  
361 with IRE1 $\alpha$  inhibitor, it remains to be elucidated whether the increased bacterial burden is  
362 due to reduced ROS generation within PMNs, less PMN recruitment, or a combination of  
363 both and warrants further investigation. IRE1 $\alpha$  deficiency has been shown to reduce  
364 bacterial killing both in *in-vivo* as well as *in-vitro* models (47) resulting in extensive liver  
365 damage in *F. tularensis* infection (27). These observations coincide with our findings of  
366 elevated bacterial burden with increased retinal tissue damage due to IRE1 $\alpha$  inhibition.

367 In summary, our study demonstrates an essential role of IRE1 $\alpha$ -mediated ER stress  
368 response in orchestrating the retinal innate immune responses in bacterial endophthalmitis.  
369 We also found that an IRE1 $\alpha$ -mediated innate immune response is regulated by TLR2,  
370 which has been shown to exert a protective effect in *S. aureus* endophthalmitis. These

371 findings uncover an important mechanism that can modulate ocular inflammation and could,  
372 therefore, provide new opportunities for the development of anti-inflammatory therapies and  
373 treatments for ocular infections.

374

## 375 **ACKNOWLEDGEMENTS**

376 This study was supported by NIH grants R01EY026964, R01EY02738, R21AI140033, and  
377 R21AI135583 (to AK). Our research is also supported in part by an unrestricted grant to the  
378 Kresge Eye Institute/Department of Ophthalmology, Visual, and Anatomical Sciences from  
379 Research to Prevent Blindness Inc. The study was partially supported by NIH grant  
380 DK090313 (to KZ). The immunology resource core is supported by an NIH center grant  
381 P30EY004068. The authors would like to thank Robert Wright for critical editing of the final  
382 manuscript. The funders had no role in study design, data collection, and interpretation, or  
383 the decision to submit the work for publication. The authors declare no conflict of interest.

## 384 **AUTHORS CONTRIBUTIONS**

385 A.K., P.K.S, and A.K. conceived the project and designed the experiments; A.K. and P.K.S.  
386 performed the experiments and analyzed the data; K.Z. and A.K. contributed reagents/  
387 materials/ analysis tools; A.K., P.K.S., and A.K. wrote the manuscript. All authors reviewed  
388 and approved the final version of the manuscript.

389

390

391 **REFERENCES**

- 392 1. Lowy, F. D. (1998) Staphylococcus aureus infections. *N Engl J Med* **339**, 520-532
- 393 2. Musher, D. M., Lamm, N., Darouiche, R. O., Young, E. J., Hamill, R. J., and Landon, G. C. (1994) The  
394 current spectrum of Staphylococcus aureus infection in a tertiary care hospital. *Medicine (Baltimore)*  
395 **73**, 186-208
- 396 3. Boucher, H., Miller, L. G., and Razonable, R. R. (2010) Serious infections caused by methicillin-  
397 resistant Staphylococcus aureus. *Clin Infect Dis* **51 Suppl 2**, S183-197
- 398 4. Talreja, D., Singh, P. K., and Kumar, A. (2015) In Vivo Role of TLR2 and MyD88 Signaling in Eliciting  
399 Innate Immune Responses in Staphylococcal Endophthalmitis. *Invest Ophthalmol Vis Sci* **56**, 1719-  
400 1732
- 401 5. Miller, F. C., Coburn, P. S., Huzzatul, M. M., LaGrow, A. L., Livingston, E., and Callegan, M. C. (2019)  
402 Targets of immunomodulation in bacterial endophthalmitis. *Prog Retin Eye Res* **73**, 100763
- 403 6. Miller, J. J., Scott, I. U., Flynn, H. W., Jr., Smiddy, W. E., Newton, J., and Miller, D. (2005) Acute-onset  
404 endophthalmitis after cataract surgery (2000-2004): incidence, clinical settings, and visual acuity  
405 outcomes after treatment. *Am J Ophthalmol* **139**, 983-987
- 406 7. Hanscom, T. (1996) The Endophthalmitis Vitrectomy Study. *Arch Ophthalmol* **114**, 1029-1030; author  
407 reply 1028-1029
- 408 8. Singh, P. K., and Kumar, A. (2015) Retinal photoreceptor expresses toll-like receptors (TLRs) and  
409 elicits innate responses following TLR ligand and bacterial challenge. *PLoS One* **10**, e0119541
- 410 9. Singh, P. K., Shiha, M. J., and Kumar, A. (2014) Antibacterial responses of retinal Muller glia:  
411 production of antimicrobial peptides, oxidative burst and phagocytosis. *J Neuroinflammation* **11**, 33
- 412 10. Kochan, T., Singla, A., Tosi, J., and Kumar, A. (2012) Toll-like receptor 2 ligand pretreatment  
413 attenuates retinal microglial inflammatory response but enhances phagocytic activity toward  
414 Staphylococcus aureus. *Infect Immun* **80**, 2076-2088
- 415 11. Kumar, A., Singh, C. N., Glybina, I. V., Mahmoud, T. H., and Yu, F. S. (2010) Toll-like receptor 2 ligand-  
416 induced protection against bacterial endophthalmitis. *J Infect Dis* **201**, 255-263
- 417 12. Coburn, P. S., Miller, F. C., LaGrow, A. L., Parkunan, S. M., Blake Randall, C., Staats, R. L., and Callegan,  
418 M. C. (2018) TLR4 modulates inflammatory gene targets in the retina during Bacillus cereus  
419 endophthalmitis. *BMC Ophthalmol* **18**, 96
- 420 13. Parkunan, S. M., Randall, C. B., Coburn, P. S., Astley, R. A., Staats, R. L., and Callegan, M. C. (2015)  
421 Unexpected Roles for Toll-Like Receptor 4 and TRIF in Intraocular Infection with Gram-Positive  
422 Bacteria. *Infect Immun* **83**, 3926-3936
- 423 14. Chang, J. H., McCluskey, P. J., and Wakefield, D. (2006) Toll-like receptors in ocular immunity and the  
424 immunopathogenesis of inflammatory eye disease. *Br J Ophthalmol* **90**, 103-108
- 425 15. Pandey, R. K., Yu, F. S., and Kumar, A. (2013) Targeting toll-like receptor signaling as a novel approach  
426 to prevent ocular infectious diseases. *Indian J Med Res* **138**, 609-619
- 427 16. Lin, J. H., Walter, P., and Yen, T. S. (2008) Endoplasmic reticulum stress in disease pathogenesis. *Annu*  
428 *Rev Pathol* **3**, 399-425
- 429 17. Xu, C., Bailly-Maitre, B., and Reed, J. C. (2005) Endoplasmic reticulum stress: cell life and death  
430 decisions. *J Clin Invest* **115**, 2656-2664
- 431 18. Yoshida, H., Matsui, T., Yamamoto, A., Okada, T., and Mori, K. (2001) XBP1 mRNA is induced by ATF6  
432 and spliced by IRE1 in response to ER stress to produce a highly active transcription factor. *Cell* **107**,  
433 881-891
- 434 19. Newton, P. M., and Ron, D. (2007) Protein kinase C and alcohol addiction. *Pharmacol Res* **55**, 570-  
435 577

- 436 20. Zhang, K., Wang, S., Malhotra, J., Hassler, J. R., Back, S. H., Wang, G., Chang, L., Xu, W., Miao, H.,  
437 Leonardi, R., Chen, Y. E., Jackowski, S., and Kaufman, R. J. (2011) The unfolded protein response  
438 transducer IRE1alpha prevents ER stress-induced hepatic steatosis. *EMBO J* **30**, 1357-1375
- 439 21. Kanemoto, S., Kondo, S., Ogata, M., Murakami, T., Urano, F., and Imaizumi, K. (2005) XBP1 activates  
440 the transcription of its target genes via an ACGT core sequence under ER stress. *Biochem Biophys Res*  
441 *Commun* **331**, 1146-1153
- 442 22. Schroder, M., and Kaufman, R. J. (2005) The mammalian unfolded protein response. *Annu Rev*  
443 *Biochem* **74**, 739-789
- 444 23. Nau, G. J., Richmond, J. F., Schlesinger, A., Jennings, E. G., Lander, E. S., and Young, R. A. (2002)  
445 Human macrophage activation programs induced by bacterial pathogens. *Proc Natl Acad Sci U S A*  
446 **99**, 1503-1508
- 447 24. Blumenthal, A., Lauber, J., Hoffmann, R., Ernst, M., Keller, C., Buer, J., Ehlers, S., and Reiling, N. (2005)  
448 Common and unique gene expression signatures of human macrophages in response to four strains  
449 of *Mycobacterium avium* that differ in their growth and persistence characteristics. *Infect Immun* **73**,  
450 3330-3341
- 451 25. Celli, J., and Tsolis, R. M. (2015) Bacteria, the endoplasmic reticulum and the unfolded protein  
452 response: friends or foes? *Nat Rev Microbiol* **13**, 71-82
- 453 26. Choi, J. A., and Song, C. H. (2019) Insights Into the Role of Endoplasmic Reticulum Stress in Infectious  
454 Diseases. *Front Immunol* **10**, 3147
- 455 27. Martinon, F., Chen, X., Lee, A. H., and Glimcher, L. H. (2010) TLR activation of the transcription factor  
456 XBP1 regulates innate immune responses in macrophages. *Nat Immunol* **11**, 411-418
- 457 28. Qiu, Q., Zheng, Z., Chang, L., Zhao, Y. S., Tan, C., Dandekar, A., Zhang, Z., Lin, Z., Gui, M., Li, X., Zhang,  
458 T., Kong, Q., Li, H., Chen, S., Chen, A., Kaufman, R. J., Yang, W. L., Lin, H. K., Zhang, D., Perlman, H.,  
459 Thorp, E., Zhang, K., and Fang, D. (2013) Toll-like receptor-mediated IRE1alpha activation as a  
460 therapeutic target for inflammatory arthritis. *EMBO J* **32**, 2477-2490
- 461 29. Rajamani, D., Singh, P. K., Rottmann, B. G., Singh, N., Bhasin, M. K., and Kumar, A. (2016) Temporal  
462 retinal transcriptome and systems biology analysis identifies key pathways and hub genes in  
463 *Staphylococcus aureus* endophthalmitis. *Sci Rep* **6**, 21502
- 464 30. Kumar, A., Giri, S., and Kumar, A. (2016) 5-Aminoimidazole-4-carboxamide ribonucleoside-mediated  
465 adenosine monophosphate-activated protein kinase activation induces protective innate responses  
466 in bacterial endophthalmitis. *Cell Microbiol* **18**, 1815-1830
- 467 31. Swamydas, M., and Lionakis, M. S. (2013) Isolation, purification and labeling of mouse bone marrow  
468 neutrophils for functional studies and adoptive transfer experiments. *J Vis Exp*, e50586
- 469 32. Singh, P. K., Donovan, D. M., and Kumar, A. (2014) Intravitreal injection of the chimeric phage  
470 endolysin Ply187 protects mice from *Staphylococcus aureus* endophthalmitis. *Antimicrob Agents*  
471 *Chemother* **58**, 4621-4629
- 472 33. Singh, S., Singh, P. K., Suhail, H., Arumugaswami, V., Pellett, P. E., Giri, S., and Kumar, A. (2020) AMP-  
473 Activated Protein Kinase Restricts Zika Virus Replication in Endothelial Cells by Potentiating Innate  
474 Antiviral Responses and Inhibiting Glycolysis. *The Journal of Immunology* **204**, 1810-1824
- 475 34. Singh, P. K., Guest, J.-M., Kanwar, M., Boss, J., Gao, N., Juzych, M. S., Abrams, G. W., Yu, F.-S., and  
476 Kumar, A. (2017) Zika virus infects cells lining the blood-retinal barrier and causes chorioretinal  
477 atrophy in mouse eyes. *JCI Insight* **2**
- 478 35. Roybal, C. N., Yang, S., Sun, C. W., Hurtado, D., Vander Jagt, D. L., Townes, T. M., and Abcouwer, S. F.  
479 (2004) Homocysteine increases the expression of vascular endothelial growth factor by a mechanism  
480 involving endoplasmic reticulum stress and transcription factor ATF4. *J Biol Chem* **279**, 14844-14852
- 481 36. Pillich, H., Loose, M., Zimmer, K. P., and Chakraborty, T. (2016) Diverse roles of endoplasmic  
482 reticulum stress sensors in bacterial infection. *Mol Cell Pediatr* **3**, 9



- 483 37. Calfon, M., Zeng, H., Urano, F., Till, J. H., Hubbard, S. R., Harding, H. P., Clark, S. G., and Ron, D. (2002)  
484 IRE1 couples endoplasmic reticulum load to secretory capacity by processing the XBP-1 mRNA.  
485 *Nature* **415**, 92-96
- 486 38. Harding, H. P., Novoa, I., Zhang, Y., Zeng, H., Wek, R., Schapira, M., and Ron, D. (2000) Regulated  
487 translation initiation controls stress-induced gene expression in mammalian cells. *Mol Cell* **6**, 1099-  
488 1108
- 489 39. Lee, A. H., Iwakoshi, N. N., and Glimcher, L. H. (2003) XBP-1 regulates a subset of endoplasmic  
490 reticulum resident chaperone genes in the unfolded protein response. *Mol Cell Biol* **23**, 7448-7459
- 491 40. Cross, B. C. S., Bond, P. J., Sadowski, P. G., Jha, B. K., Zak, J., Goodman, J. M., Silverman, R. H., Neubert,  
492 T. A., Baxendale, I. R., Ron, D., and Harding, H. P. (2012) The molecular basis for selective inhibition  
493 of unconventional mRNA splicing by an IRE1-binding small molecule. *Proceedings of the National*  
494 *Academy of Sciences* **109**, E869-E878
- 495 41. Liao, K., Guo, M., Niu, F., Yang, L., Callen, S. E., and Buch, S. (2016) Cocaine-mediated induction of  
496 microglial activation involves the ER stress-TLR2 axis. *J Neuroinflammation* **13**, 33
- 497 42. Coope, A., Milanski, M., Arruda, A. P., Ignacio-Souza, L. M., Saad, M. J., Anhe, G. F., and Velloso, L. A.  
498 (2012) Chaperone insufficiency links TLR4 protein signaling to endoplasmic reticulum stress. *J Biol*  
499 *Chem* **287**, 15580-15589
- 500 43. Zhong, Y., Li, J., Chen, Y., Wang, J. J., Ratan, R., and Zhang, S. X. (2012) Activation of endoplasmic  
501 reticulum stress by hyperglycemia is essential for Muller cell-derived inflammatory cytokine  
502 production in diabetes. *Diabetes* **61**, 492-504
- 503 44. Kumar, A., Yin, J., Zhang, J., and Yu, F. S. (2007) Modulation of corneal epithelial innate immune  
504 response to pseudomonas infection by flagellin pretreatment. *Invest Ophthalmol Vis Sci* **48**, 4664-  
505 4670
- 506 45. Kim, H. T., Qiang, W., Liu, N., Scofield, V. L., Wong, P. K., and Stoica, G. (2005) Up-regulation of  
507 astrocyte cyclooxygenase-2, CCAAT/enhancer-binding protein-homology protein, glucose-related  
508 protein 78, eukaryotic initiation factor 2 alpha, and c-Jun N-terminal kinase by a neurovirulent  
509 murine retrovirus. *J Neurovirol* **11**, 166-179
- 510 46. Cao, S. S., and Kaufman, R. J. (2014) Endoplasmic reticulum stress and oxidative stress in cell fate  
511 decision and human disease. *Antioxid Redox Signal* **21**, 396-413
- 512 47. Abuaita, B. H., Burkholder, K. M., Boles, B. R., and O'Riordan, M. X. (2015) The Endoplasmic Reticulum  
513 Stress Sensor Inositol-Requiring Enzyme 1alpha Augments Bacterial Killing through Sustained  
514 Oxidant Production. *mBio* **6**, e00705
- 515 48. Ozgur, R., Uzilday, B., Iwata, Y., Koizumi, N., and Turkan, I. (2018) Interplay between the unfolded  
516 protein response and reactive oxygen species: a dynamic duo. *J Exp Bot* **69**, 3333-3345
- 517 49. Senft, D., and Ronai, Z. A. (2015) UPR, autophagy, and mitochondria crosstalk underlies the ER stress  
518 response. *Trends Biochem Sci* **40**, 141-148
- 519 50. Chen, S., and Zhang, D. (2015) Friend or foe: Endoplasmic reticulum protein 29 (ERp29) in epithelial  
520 cancer. *FEBS Open Bio* **5**, 91-98
- 521 51. Cunard, R. (2015) Endoplasmic Reticulum Stress in the Diabetic Kidney, the Good, the Bad and the  
522 Ugly. *J Clin Med* **4**, 715-740
- 523 52. Smith, J. A., Khan, M., Magnani, D. D., Harms, J. S., Durward, M., Radhakrishnan, G. K., Liu, Y. P., and  
524 Splitter, G. A. (2013) Brucella induces an unfolded protein response via TcpB that supports  
525 intracellular replication in macrophages. *PLoS Pathog* **9**, e1003785
- 526 53. Qin, Q. M., Pei, J., Ancona, V., Shaw, B. D., Ficht, T. A., and de Figueiredo, P. (2008) RNAi screen of  
527 endoplasmic reticulum-associated host factors reveals a role for IRE1alpha in supporting Brucella  
528 replication. *PLoS Pathog* **4**, e1000110
- 529 54. Kroeger, H., Chiang, W. C., Felden, J., Nguyen, A., and Lin, J. H. (2019) ER stress and unfolded protein  
530 response in ocular health and disease. *FEBS J* **286**, 399-412

- 531 55. Zode, G. S., Sharma, A. B., Lin, X., Searby, C. C., Bugge, K., Kim, G. H., Clark, A. F., and Sheffield, V. C.  
532 (2014) Ocular-specific ER stress reduction rescues glaucoma in murine glucocorticoid-induced  
533 glaucoma. *The Journal of Clinical Investigation* **124**, 1956-1965
- 534 56. Bhatta, M., Chatpar, K., Hu, Z., Wang, J. J., and Zhang, S. X. (2018) Reduction of Endoplasmic  
535 Reticulum Stress Improves Angiogenic Progenitor Cell function in a Mouse Model of Type 1 Diabetes.  
536 *Cell Death Dis* **9**, 467-467
- 537 57. Webster, S. J., Ellis, L., O'Brien, L. M., Tyrrell, B., Fitzmaurice, T. J., Elder, M. J., Clare, S., Chee, R.,  
538 Gaston, J. S., and Goodall, J. C. (2016) IRE1alpha mediates PKR activation in response to Chlamydia  
539 trachomatis infection. *Microbes Infect* **18**, 472-483
- 540 58. de Jong, M. F., Starr, T., Winter, M. G., den Hartigh, A. B., Child, R., Knodler, L. A., van Dijl, J. M., Celli,  
541 J., and Tsolis, R. M. (2013) Sensing of bacterial type IV secretion via the unfolded protein response.  
542 *mBio* **4**, e00418-00412
- 543 59. Morinaga, N., Yahiro, K., Matsuura, G., Moss, J., and Noda, M. (2008) Subtilase cytotoxin, produced  
544 by Shiga-toxigenic Escherichia coli, transiently inhibits protein synthesis of Vero cells via degradation  
545 of BiP and induces cell cycle arrest at G1 by downregulation of cyclin D1. *Cell Microbiol* **10**, 921-929
- 546 60. Pillich, H., Loose, M., Zimmer, K. P., and Chakraborty, T. (2012) Activation of the unfolded protein  
547 response by Listeria monocytogenes. *Cell Microbiol* **14**, 949-964
- 548 61. Dandekar, A., Qiu, Y., Kim, H., Wang, J., Hou, X., Zhang, X., Zheng, Z., Mendez, R., Yu, F. S., Kumar, A.,  
549 Fang, D., Sun, F., and Zhang, K. (2016) Toll-like Receptor (TLR) Signaling Interacts with CREBH to  
550 Modulate High-density Lipoprotein (HDL) in Response to Bacterial Endotoxin. *J Biol Chem* **291**, 23149-  
551 23158
- 552 62. Osowski, C. M., Hara, T., O'Sullivan-Murphy, B., Kanekura, K., Lu, S., Hara, M., Ishigaki, S., Zhu, L. J.,  
553 Hayashi, E., Hui, S. T., Greiner, D., Kaufman, R. J., Bortell, R., and Urano, F. (2012) Thioredoxin-  
554 interacting protein mediates ER stress-induced beta cell death through initiation of the  
555 inflammasome. *Cell Metab* **16**, 265-273
- 556 63. Chong, W. C., Shastri, M. D., and Eri, R. (2017) Endoplasmic Reticulum Stress and Oxidative Stress: A  
557 Vicious Nexus Implicated in Bowel Disease Pathophysiology. *Int J Mol Sci* **18**

558

559

560

561

562

563

564

565

566

567

568

569

# Author Manuscript

570 **FIGURE LEGENDS**

571 **Figure 1. *S. aureus* infection induces ER stress in the mouse retina.** C57BL/6 mouse  
572 (n=6) eyes were intravitreally injected with PBS (control, C) or 5000 CFU of *S. aureus* (SA),  
573 strain RN6390. At indicated time point post-infection, eyes were enucleated, and retinal  
574 tissue was subjected to temporal transcriptomic analysis using microarray (reported  
575 previously (29)). The microarray data showed induced expression of *Xbp1* and *Bip* genes.  
576 The data are expressed as relative fold change by normalizing the expression of genes with  
577 respect to control **(A)**. In another set of experiments, RNA was extracted from SA-infected  
578 retinal tissue at 24h and subjected to RT-PCR to detect mRNA expression of indicated ER  
579 stress markers **(B)**. Results are representative of at least two independent (n=6 each)  
580 experiments. Statistical analysis was performed using one-way ANOVA \*,  $P < 0.05$ ; \*\*,  $P <$   
581 0.001. Data are shown as the mean  $\pm$  SD

582 **Figure 2. *S. aureus* induces IRE1 $\alpha$  mediated ER stress via TLR2.** C57BL/6 (WT), TLR2<sup>-</sup>  
583 <sup>-</sup>, and MyD88<sup>-</sup> mouse (n=6 each) (all on B6 background) eyes were intravitreally injected  
584 with 4 $\mu$ 8C (0.1 $\mu$ g/eye), 12h post drug injection, SA endophthalmitis was induced, and retinal  
585 tissue (24h post-SA infection) was harvested and subjected to RT-PCR to detect IRE1 $\alpha$   
586 expression and XBP1 splicing, using GAPDH as housekeeping gene **(A)**. The protein levels  
587 of pIRE1 $\alpha$  and IRE1 $\alpha$  were assessed by western blot **(B, left panel)**, and band intensities  
588 were quantified using ImageJ, normalized with  $\beta$ -actin, and represented as a bar graph **(B,**  
589 **Right panel)**. Mouse microglial cells (BV2 cell line) were left untreated or pre-treated with  
590 IRE1 $\alpha$  inhibitor, 4 $\mu$ 8C (100 nM), followed by challenge with *S. aureus* (SA), TLR2 agonist  
591 (Pam3CSK4, 10  $\mu$ g/ml), and, TLR4 agonist (LPS, 10  $\mu$ g/ml) for 8h. The mRNA expression

592 of indicated ER stress markers was assessed by RT-PCR **(C)**. The protein levels of pIRE1 $\alpha$   
593 and IRE1 $\alpha$  were assessed by western blot **(D, left panel)**, and band intensities were  
594 quantified using ImageJ, normalized with  $\beta$ -actin, and represented as a bar graph **(D, Right**  
595 **panel)** Results are representative of at least three independent experiments. Statistical  
596 analysis was performed using one-way ANOVA \*,  $P < 0.05$ ; \*\*,  $P < 0.01$ ; \*\*\*\*,  $P < 0.0001$ ; ns,  
597 not significant.

598 **Figure 3. IRE1 $\alpha$  regulates *S. aureus* and TLR2 ligand-induced inflammatory response.**

599 C57BL/6 (WT) and TLR2<sup>-/-</sup> mouse (n = 6 per group) eyes were injected with IRE1 $\alpha$  inhibitor,  
600 4 $\mu$ 8C (0.1  $\mu$ g/eye), 12h prior to induction of *S. aureus* endophthalmitis and at 24h post-  
601 infection eye lysates were subjected to ELISA for measurements of indicated  
602 cytokines/chemokines **(A)**. BV2 microglial cells were pre-treated with 4 $\mu$ 8C (100 nM, for 1h)  
603 followed by challenge with SA (MOI 10:1), and Pam3CSK4 (10  $\mu$ g/ml) for 8h. The  
604 conditioned media was used for ELISA for the quantification of indicated  
605 cytokines/chemokines **(B)**. The production of inflammatory mediators was assessed in  
606 IRE1 $\alpha$ <sup>flox/flox</sup>, and myeloid cell-specific IRE1 $\alpha$ <sup>-/-</sup> BMDM (M $\Phi$ ) challenged with SA (MOI 10:1)  
607 for 8h using ELISA **(C)**. Results are cumulative of at least two independent (n=6 each)  
608 experiments. Statistical analysis was performed using Student's t-test \*,  $P < 0.05$ ; \*\*,  $P < 0.01$ ;  
609 \*\*\*,  $P < 0.001$ ; \*\*\*\*,  $P < 0.0001$ ; ns, not significant. Data are shown as the mean  $\pm$  SD.

610 **Figure 4. IRE1 $\alpha$  inhibition attenuates *S. aureus* induced NF- $\kappa$ B and MAPK signaling.**

611 C57BL/6 mouse (n = 6 per group) eyes were injected with IRE1 $\alpha$  inhibitor, 4 $\mu$ 8C (0.1  
612  $\mu$ g/eye), 12h prior to the induction of *S. aureus* (SA) endophthalmitis. At 24h post-infection,  
613 retinal tissue lysates were subjected to western blot analysis for pI $\kappa$ B, pERK, and pp38

614 signaling pathways (**A, Left panel**). Band intensities were quantified using ImageJ,  
615 normalized with  $\beta$ -actin, and represented as fold change in a bar graph (**A, Right panel**).  
616 BV2 cells were pre-treated for 1h with NF- $\kappa$ B, p38, and ERK inhibitors (10  $\mu$ M each) followed  
617 by SA (MOI 10:1) challenge for 8h. Total RNA was extracted, reverse transcribed, and  
618 subjected to RT-PCR for XBP1 spliced (XBP1s) and unspliced (XBP1u) forms. Statistical  
619 analysis was performed using one-way ANOVA. Data represent mean  $\pm$  SD. from two  
620 independent (n=6 each) experiments \*,  $P < 0.05$ ; \*\*,  $P < 0.01$ ; \*\*\*,  $P < 0.001$ .

621 **Figure 5. ROS inhibition reduces *S. aureus* induced XBP1 splicing and inflammatory**  
622 **mediators.** BV2 microglial cells were left untreated or pre-treated with NADPH oxidase  
623 inhibitor, DPI (1  $\mu$ M) for 1h followed by *S. aureus* (SA) challenge for 8 h. Total RNA was  
624 extracted, reverse transcribed, and subjected to RT-PCR for detection of IRE1 $\alpha$  and XBP1  
625 (unspliced: XBPu, spliced: XBP<sub>s</sub>) (**A**). ELISA was performed from conditioned media for  
626 indicated cytokines/chemokines quantification (**B**). Results are cumulative of at least three  
627 independent experiments. Statistical analysis was performed using Student's t-test, \*\*\*\*,  
628  $P < 0.0001$ . Data are shown as the mean  $\pm$  SD.

629 **Figure 6. IRE1 $\alpha$  inhibition aggravates disease pathology in mouse eyes.** Eyes of  
630 C57BL/6 WT mouse (n = 6) were pre-treated by intravitreal injection with 4 $\mu$ 8C (0.1  $\mu$ g/eye),  
631 followed by induction of *S. aureus* (SA) endophthalmitis. Twenty-four hours post-SA  
632 infection, eyes were enucleated, lysate was prepared in sterile PBS, and the bacterial count  
633 was measured by serial plate dilution and represented as CFU per eye (**A**). Histological  
634 analysis was performed at 24h post-infection by paraffin embedding and H&E staining.  
635 4 $\mu$ 8C alone injected eyes were used as control (**B**). Retinal cell death was visualized by

636 TUNEL staining on cryosections showing TUNEL-positive cells (green) and DAPI stained  
637 nuclei (blue) (**C**). Flow cytometry was used to assess PMN infiltration by pooling retina from  
638 two eyes and staining single-cell suspensions with anti-CD45-PECy5 and anti-Ly6G-FITC  
639 monoclonal antibodies (**D**). Representative dot plots show the percentage of dually positive  
640 PMNs (upper right quadrants in **upper panel**). The bar graph shows cumulative quantitative  
641 data from three independent experiments (**lower panel**). (ONH: optic nerve head, RPE:  
642 retinal pigmented epithelium layer, ONL: outer nuclear layer, INL: inner nuclear layer, GCL:  
643 ganglion cell layer, VC: vitreous chamber, L: lens) Statistical analysis was performed using  
644 Student's t-test. Data represent mean  $\pm$  SD from two independent (n=6 each) experiments  
645 \*\*,  $P < 0.01$ .

646 **Figure 7. A schematic illustration of IRE1 $\alpha$  in regulating the innate inflammatory**  
647 **response in bacterial endophthalmitis.** TLR2 recognizes *S. aureus* and induces IRE1 $\alpha$   
648 activation through ROS generation. This causes splicing of IRE1 $\alpha$  downstream target,  
649 XBP1, which activates NF- $\kappa$ B and MAPK signaling resulting in the production of pro-  
650 inflammatory cytokines/chemokines. *S. aureus* infection primarily induces, IRE1 $\alpha$ -XBP1  
651 axis of the ER stress response. The schematic diagram was created using BioRender  
652 software.

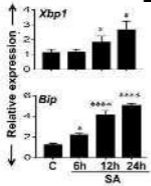
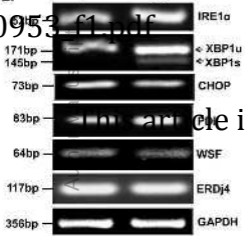
653

654

655

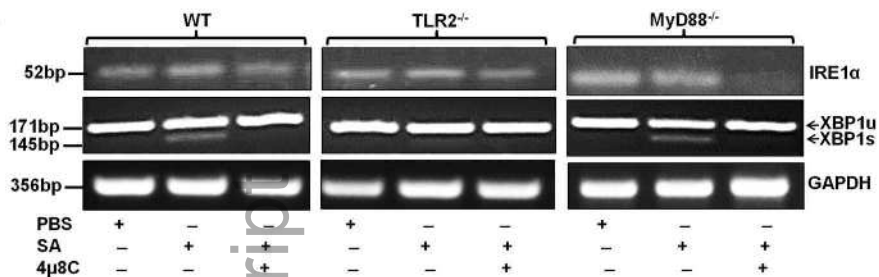
**A.**

fsb2\_20953\_f1.pdf

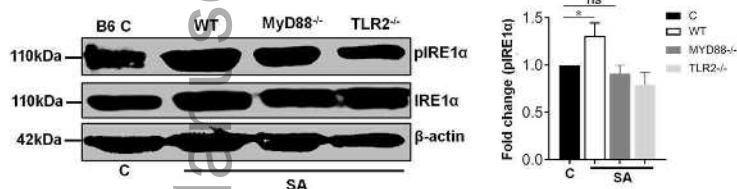
**B.**



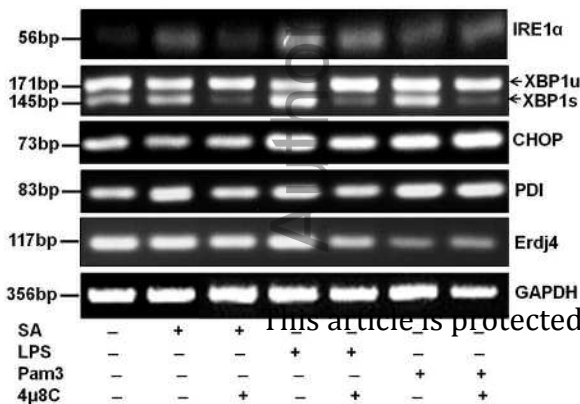
A.



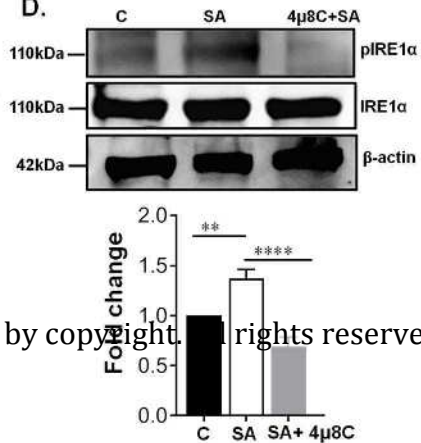
B.



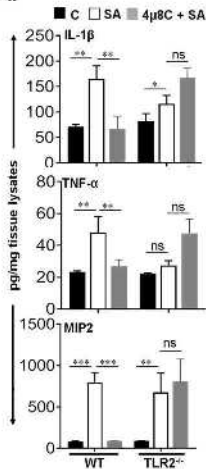
C.



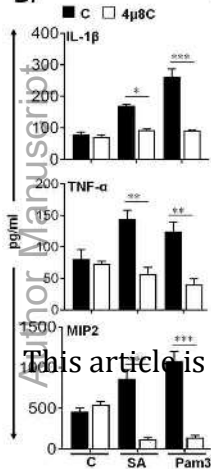
D.



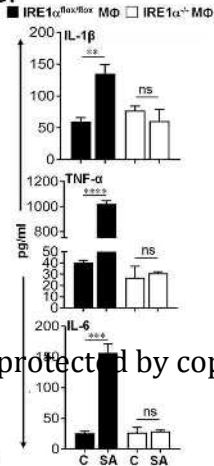
A.



B.

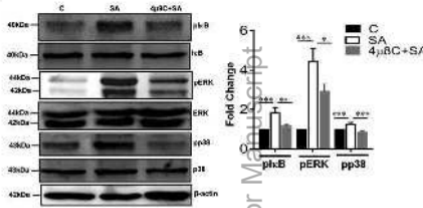


C.

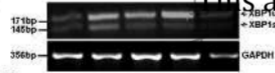


This article is protected by copyright

A.



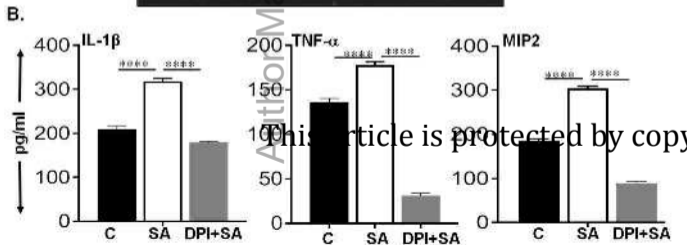
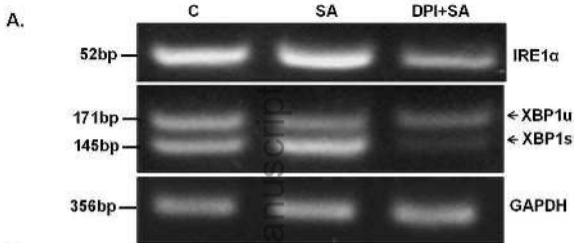
B.

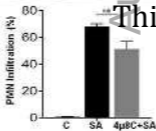
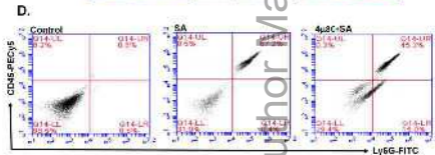
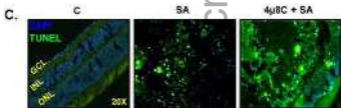
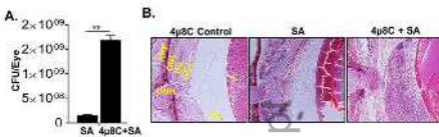


SA	-	+	+	+	+
NF-κB inh.	-	-	+	+	-
p38 Inh.	-	-	-	+	-
ERK inh.	-	-	-	-	+

This article is

Dr Manuscript





This article is

*S. aureus*

TLR2



ROS



UPR response



ER



XBP1u



XBP1s



NF- $\kappa$ B/  
MAPK

Cytokines

Chemokines



Author Manuscript